J|A|C|S
ARTICLES
Published on Web 02/07/2002

Development and Validation of an Integrated Computational Approach for the Study of Ionic Species in Solution by Means of Effective Two-Body Potentials. The Case of Zn^{2+}, Ni^{2+}, and Co^{2+} in Aqueous Solutions

Giovanni Chillemi,*[,§] Paola D'Angelo,*[,†,||] Nicolae Viorel Pavel,[†] Nico Sanna,[§] and Vincenzo Barone[‡]

Contribution from CASPUR, c/o Università di Roma "La Sapienza", P.le Aldo Moro 5, 00185 ROMA, Italy, and Dipartimento di Chimica, Università di Roma "La Sapienza", P.le Aldo Moro 5, 00185 ROMA, Italy, and Dipartimento di Chimica, Università di Napoli "Federico II", Complesso Universitario di Monte S. Angelo, Via Cintia, 80126 NAPOLI, Italy, INFM UdR CM, Dipartimento di Chimica, Universitá di Napoli "Federico II", Complesso Universitario di Monte S. Angelo Via Cintia, 80126 NAPOLI, Italy

Received February 17, 2001. Revised Manuscript Received September 18, 2001

Abstract: In this paper we have developed an effective computational procedure for the structural and dynamical investigation of ions in aqueous solutions. Quantum mechanical potential energy surfaces for the interaction of a transition metal ion with a water molecule have been calculated taking into account the effect of bulk solvent by the polarizable continuum model (PCM). The effective ion−water interactions have been fitted by suitable analytical potentials, and have been utilized in molecular dynamics (MD) simulations to obtain structural and dynamical properties of the ionic aqueous solutions. This procedure has been successfully applied to the $Co^{2+}-H_2O$ open-shell system and, for the first time, Co−oxygen and Co−hydrogen pair potential functions have been determined and employed in MD simulations. The reliability of the whole procedure has been assessed by applying it also to the Zn^{2+} and Ni^{2+} aqueous solutions, and the structural and dynamical properties of the three systems have been calculated by means of MD simulations and have been found to be in very good agreement with experimental results. The structural parameters of the first solvation shells issuing from the MD simulations provide an effective complement to extended X-ray absorption fine structure (EXAFS) experiments.

1. Introduction

Our knowledge of the coordination of aqua-ions has been greatly increased over the past decades, due to the availability of more accurate experimental data[1] and to the refinement of the theoretical models used to describe the ion−water interaction.[2−8] Among the different computational approaches, molecular dynamics (MD) represents an essential instrument for casting light on the structure of the first and second coordination shells of aqueous solutions, besides giving information on thermodynamic and dynamic properties of these systems. More recently, MD simulations have been used as an aid in obtaining accurate structural information from the extended X-ray absorption fine structure (EXAFS) data.[9,10] However, classical MD simulations require analytical potentials describing the interactions among different atoms. In this context, aqueous solutions represent, of course, the most important target and the accurate description of water−water interactions is a mandatory prerequisite for their simulation. As a consequence much effort has been made to produce reliable ab initio potential energy surfaces for water[11,12] which were fitted with two-, three-, or four-body analytical functions to correctly include induction forces in the intermolecular interaction energy.[3] Next, the effort has been shifted to ion−water potentials following two different strategies. The first approach relies on the direct fitting of suitable experimental data by empirical potentials.[2] Alternatively, MD force field parametrizations for the hydrated metal ion have been carried out through quantum mechanical ab initio calculations, using different computational strategies. In particular two methods are worth mentioning. The

§ CASPUR.
† Università di Roma "La Sapienza".
‡ Università di Napoli "Federico II".
|| INFM UdR CM.

(1) Ohtaki, H.; Radnai, T. *Chem. Rev.* **1993**, *93*, 1157.
(2) Aqvist, J. *J. Phys. Chem.* **1990**, *94*, 8021.
(3) Saint-Martin, H.; Medina-Llanos, C.; Ortega-Blake, I. *J. Chem. Phys.* **1990**, *93*, 6448.
(4) Floris, F.; Persico, M.; Tani, A.; Tomasi, J. *Chem. Phys. Lett.* **1992**, *199*, 518.
(5) Floris, F.; Persico, M.; Tani, A.; Tomasi, J. *Chem. Phys.* **1995**, *195*, 207.
(6) Marini, G. W.; Texler, R.; Rode, B. M. *J. Phys. Chem.* **1996**, *100*, 6808.
(7) Periole, X.; Allouche, D.; Daudey, J.-P.; Sanejouand, Y.-H. *J. Phys. Chem. B* **1997**, *101*, 5018.
(8) Martìnez, J. M.; Pappalardo, R. R.; Marcos, E. S. *J. Chem. Phys.* **1998**, *109*, 1445.
(9) D'Angelo, P.; Di Nola, A.; Filipponi, A.; Pavel, N. V.; Roccatano, D. *J. Chem. Phys.* **1994**, *100*, 985.
(10) Roccatano, D.; Berendsen, H. J. C.; D'Angelo, P. *J. Chem. Phys.* **1998**, *108*, 9487.
(11) Clementi, E.; Corongiu, G. *Int. J. Quantum Chem. Quantum Biol. Symp.* **1983**, *10*, 31.
(12) Huang, M. J.; Dupuis, M.; Niesar, U.; Corongiu, G.; Clementi, E. *Int. J. Quantum Chem. Quantum Chem. Symp.* **1989**, *23*, 421.

10.1021/ja015686p CCC: $22.00

first approach adds three-body contributions to the ab initio ion−water potential obtained in vacuo.[6] According to the second method, ab initio calculations are carried out on a system consisting either of the ion with its first hydration shell only[7] or of a second shell water molecule that directly interacts with the hydrated ion.[8]

The aim of the present work is to develop, within the framework of ab initio approaches, a reproducible self-consistent computational procedure able to generate ion−water force fields which can be implemented in MD codes. Structural results obtained from MD simulations are used as starting models in the EXAFS analysis of Zn^{2+}, Ni^{2+}, and Co^{2+} water solutions and the comparison of theoretical and experimental results provides a useful test of the reliability of the entire procedure. The computational protocol consists of three main steps: (i) generation of ab initio potential energy surfaces (PES); (ii) PES fitting and potential parameter evaluation; and (iii) MD code modification, simulations, and analysis.

In section 2 we will give the essential details of this computational procedure while in section 3 we will report the results issuing from MD simulations employing our new effective potentials.

2. The Computational Procedure

Although the basic aspects of our computational model are well established, a number of methodological and numerical improvements have been introduced, which led to a reproducible user-friendly procedure. The choice of a three-step calculation scheme arises from the experiences gathered by many groups involved in this field.

In step (i) of the analysis we use the method proposed by Floris et al.[4,5] to calculate an effective pair potential between one water molecule and an ion solvated by means of the polarizable continuum model (PCM).[13] Due to recent improvements and optimizations of the PCM and its inclusion as a computational tool in the Gaussian98 package,[14] the ab initio PES can be generated very efficiently for molecular systems such as $M^{n+}-H_2O$. The validity of this approach, as compared to the calculation on clusters of the type $[M(H_2O)_m]^{n+}$, has been previously assessed,[4] and its main advantage is that this procedure does not need the a priori knowledge of the hydration number of the ion. Note that, very often, a correct hydration number is obtained only by using the PCM method, while in vacuo modeling of the interaction results in an underestimation of the coordination number. For example, in the case of Zn^{2+} the in vacuo calculations lead to a hydration number of four,[15] while the bulk solvent effects introduced by the PCM model induce a preference for an octahedral coordination around the ion. This effect has been recently shown also in the case of lanthanide hydration.[16] Moreover, these ab initio calculations are less computationally expensive compared to other methods, since only one explicit water molecule is used, and the number of PES points to be calculated is strongly reduced for symmetry reasons.

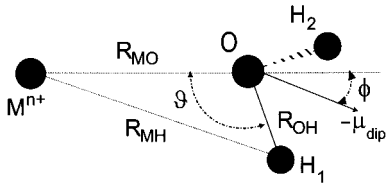

Figure 1. $M^{n+}-H_2O$ geometrical parameter definition. The $M\hat{O}H_1$ angle θ is defined in the plane containing the M^{n+}, O, and H_1 atoms. μ_{dip} is the dipole water moment. The tilt angle ϕ is the angle between the $M^{n+}-O$ and the water dipole moment directions.

In step (ii) the PES is fitted with a suitable functional form of the ion−water interaction potential. This second stage greatly benefits from the simple $M^{n+}-H_2O$ 1−1 interaction model adopted in the preceding phase. Note that the fitting procedures have been carried out keeping fixed the oxygen and hydrogen atomic charges to the values of the SPC/E water model.[17]

In step (iii) the ion−water potential described above is included in the GROMACS MD code[18] using the SPC/E potential for the water−water interactions. As a consequence, all the water molecules are described by the same potentials, in contrast to other methods where the first shell and the bulk water molecules are treated in a different way, thus requiring the a priori knowledge of the ionic coordination number.[7,8]

2.1. Step I: Generation of ab Initio PES. As mentioned above, in the first step of our procedure an effective ion−water pair potential function (U_{MW}) is calculated over a suitable grid according to the method proposed by Floris et al.[4,5] In the case of a M^{n+} ion and a water molecule W, the expression for U_{MW} is:

$$U_{MW} = \langle\psi|\hat{\mathscr{H}}^{(0)}|\psi\rangle_{MW} - \langle\psi|\hat{\mathscr{H}}^{(0)}|\psi\rangle_{M} - \langle\psi|\hat{\mathscr{H}}^{(0)}|\psi\rangle_{W} \quad (1)$$

where the wave function ψ is perturbed by the solvent effect according to the PCM, while the Hamiltonian operators $\hat{\mathscr{H}}^{(0)}$ are those of the $M^{n+}-H_2O$, bare M^{n+} ion, and bare water molecule in vacuo, respectively. No pair interactions between the explicit water molecule and the other solvent molecules are included, since they will be taken into account in the MD simulations.

The U_{MW} has been evaluated using the recent implementation of the PCM present in the Gaussian98 package by means of several *scan* jobs along the ion−oxygen distance (R_{MO}), with variable $\angle MOH$ angles (θ), generating a (R_{MO}, θ) grid (see Figure 1).

A first significant difference between our procedure and previous approaches is our choice of a single determinant model for the quantum mechanical computations. In pursuit of a computationally feasible one-determinant description of the $M^{n+}-H_2O$ interaction also for open-shell systems, we found Restricted open-shell Hartree−Fock (ROHF) to be the most balanced method for describing the molecular systems under study. The reason for this choice is many-fold: (i) the ROHF approach offers a better long-range description of the molecular S^2 spin state with respect to the unrestricted Hartree−Fock (UHF) method; (ii) in contrast to many density functionals, the ROHF model is well behaved even in the repulsive and asymptotic interaction regions, far from the energy minimum; and (iii) the ROHF, being a single determinant model, can be used to calculate ab initio energies efficiently even in difficult regions of the $M^{n+}-H_2O$ interaction, where several points of the (R_{MO}, θ) grid are needed.

The coupling of the ROHF method with a self-consistent reaction field (SCRF) modeling of the solute−solvent interactions via the PCM is one of the key features of our computational protocol. While the original version of the model was employed in previous investigations,

(13) Amovilli, C.; Barone, V.; Cammi, R.; Cances, E.; Cossi, M.; Mennucci, B.; Pomelli, C. S.; Tomasi, J. *Adv. Quantum Chem.* **1999**, *32*, 227.
(14) Frish, M. J.; Trucks, G. W.; Schlegel, H. B.; Scuseria, G. E.; Robb, M. A.; Cheesman, J. R.; Zakrrewsky, V. G.; Montgomery, J. A.; Stratmann, R. E.; Burant, J. C.; Dapprich, S.; Millam, J. M.; Daniels, A. D.; Kudin, K. N.; Strain, M. C.; Farkas, O.; Tomasi, J.; Barone, V.; Cossi, M.; Cammi, R.; Menucci, B.; Pomelli, C.; Adamo, C.; Clifford, S.; Ochtersky, J.; Petersson, G. A.; Ayala, P. Y.; Cui, Q.; Morokuma, K.; Malick, D. K.; Rabuck, A. D.; Raghavachari, K.; Foresman, J. B.; Cioslowsky, J.; Ortiz, J. V.; Stefanov, B. B.; Liu, G.; Liashenko, A.; Piskorz, P.; Komaromi, I.; Gomperts, R.; Martin, R. L.; Fox, D. J.; Keith, T.; Al-Laham, M. A.; Peng, C. Y.; Nanayakkara, A.; Gonzales, C.; Challacombe, M.; Gill, P. M. W.; Johnson, B. G.; Chen, W.; Wong, M. W.; Andres, J. L.; Head-Gordon, M.; Replogle, E. S.; Pople, J. A. *Gaussian 98 (Revision A.7)*; Gaussian Inc.: Pittsburgh, 1998.
(15) Pavlov, M.; Siegbahn, P. E. M.; Sandström, M. *J. Phys. Chem. A* **1998**, *102*, 219.
(16) Cosentino, U.; Villa, A.; Pitea, D.; Moro, G.; Barone, V. *J. Phys. Chem. B* **2000**, *104*, 8001.
(17) Berendsen, H. J. C.; Grigera, J. R.; Straatsma, T. P. *J. Phys. Chem.* **1987**, *91*, 6269.
(18) Berendsen, H. J. C.; van der Spool, D.; van Drunen, R. *Comput. Phys. Commun.* **1995**, *91*, 43.

Table 1. Comparison of Water Charge Distribution and Dipole Moment Calculated at RHF and B3LYP Levels with the cc-pVTZ Basis Set vs the SPC/E Force-Field

method	O charge (au)	H charge (au)	dipole (D)
Vacuo RHF	−0.737	+0.369	2.025
CPCM RHF	−0.854	+0.427	2.364
Vacuo B3LYP	−0.699	+0.350	1.918
CPCM B3LYP	−0.819	+0.410	2.265
SPC/E	−0.848	+0.424	2.351

here we adopted the CPCM variant[19,20] for the inclusion of the solvent effects in the bare ion−water system. This approach is strictly related, although not identical, to the so-called COSMO model[21,22] and provides results very close to those obtained by the original dielectric PCM[13] for high dielectric constant solvents. Note that this procedure is less prone to numerical errors arising from the numerical integration and from the small part of the solute electron cloud lying outside the cavity (escaped charge effects).[19−23]

Another leading factor that affects the accuracy of these as well as almost all quantum chemistry calculations is the choice of the basis set. We decided to employ the LANL2DZ effective core potentials (ECP's) and valence basis sets[24−26] for the Zn^{2+}, Ni^{2+}, and Co^{2+} central ions due to their reliability in the description of the atomic properties of heavy elements including scalar relativistic effects.[26] Furthermore, the LANL2DZ model for light transition metals has only 10 core electrons replaced by an ECP, whereas all the electrons with principal quantum numbers equal to 3 or 4 are explicitly taken into account using a double-ζ basis set of contracted Gaussian functions.

Regarding the description of the water molecule, we decided to select a basis set that is able to reproduce, as accurately as possible, the charge distribution of the SPC/E force field which will be employed in the MD simulations. To this end, we carried out several quantum mechanical energy calculations and charge fittings of the molecular electrostatic potential by the CHelpG procedure[27] implemented in the Gaussian package. We used the Hartree−Fock and Becke three-parameter Lee/Yang/Parr−B3LYP−density functional methods[28,29] with the cc-pVTZ basis set.[30] The water geometry chosen refers to the experimental R_{OH} distance of 0.9575 Å and the $\angle HOH$ angle of 104.51°, which have been used in the derivation of different water pair potentials (e.g., see ref 17). In Table 1 we report the final results of the water charge distribution which show the excellent agreement between our CPCM calculations and the GROMACS SPC/E force field.

A second important methodological issue concerns the electron spin state of the $M^{n+}-H_2O$ system with respect to the single chemical species involved in the interaction. Even if we limited the calculation to the 1−1 pair interaction between the ion and a single water molecule, thus not including any many-body treatment, some significant results are worth being pointed out. Table 2 shows the results of the energy calculations performed in vacuo and with the CPCM method, for the isolated ions and for the $M^{n+}-H_2O$ systems. Note that in these calculations the ions were coplanar with the water molecule, the R_{MO} distances were kept fixed at 2.4 Å, and the θ angle was 127.745° (see Figure 1).

The simplest case is represented by the Zn^{2+} ion where the ground electronic state is a singlet both for the isolated ion and for the $Zn^{2+}-H_2O$ system. This behavior changes significantly in the case of Ni^{2+}: while for the isolated ion the triplet is more stable than the singlet spin state, in the complexed form the singlet and triplet states are nearly isoenergetic even though a stabilization of the singlet state is found in the CPCM computations. In the case of the $Co^{2+}-H_2O$ system the quartet state is more stable than the doublet one, thus confirming the energetics of the isolated Co^{2+} ion. This finding has imposed a more accurate analysis of the electronic state of the $Ni^{2+}-$ and $Co^{2+}-H_2O$ systems in a wide distance range (1.2−4.0 Å) and θ equal to 127.745°, keeping the ions coplanar with the water molecule. In this configuration the two water hydrogen atoms are at the maximum distance from the ion and this corresponds to the minimum energy of the system. The results of these calculations (see Figure 2) show that in the case of Ni^{2+} the singlet state is more stable than the triplet one in the whole distance range. As far as the Co^{2+} ion is concerned the quartet state is more stable than the doublet one for distances longer than about 1.7 Å, while they are nearly isoenergetic in the repulsive region.

Table 2. Total Energies of the Bare Ions and $Zn^{2+}-$, $Ni^{2+}-$, and $Co^{2+}-H_2O$ Pairs in Vacuo and with Use of the CPCM Method

ion/spin state	vacuo (au)		CPCM (au)	
	$E(M^{2+})$	$E(M^{2+}-H_2O)$	$E(M^{2+})$	$E(M^{2+}-H_2O)$
Zn singlet	−62.637	−138.802	−63.600	−139.640
triplet	−62.248	−138.715	−63.315	−139.341
Ni singlet	−167.274	−243.439	−168.257	−244.293
triplet	−167.343	−243.468	−168.326	−244.037
Co doublet	−143.083	−219.358	−144.077	−220.217
quartet	−143.256	−219.480	−144.241	−220.340

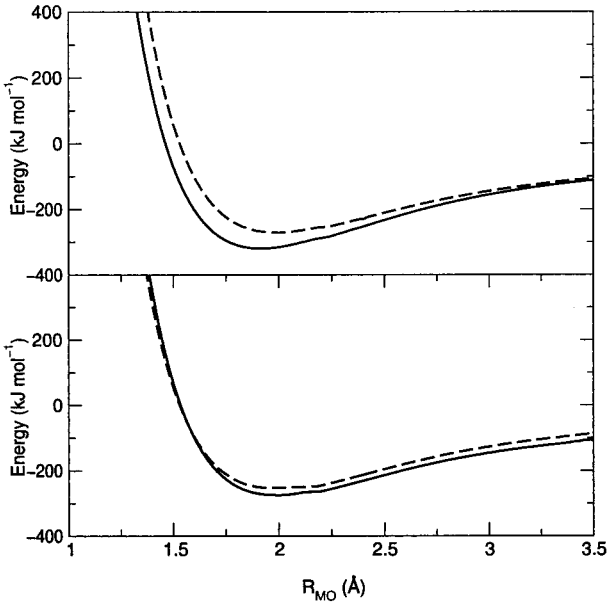

Figure 2. $M^{n+}-H_2O$ interaction energy curves vs the ion−oxygen (R_{MO}) distance for Ni^{2+} and Co^{2+} ions. Upper panel: the Ni^{2+} singlet and triplet spin states are represented as a solid line and a dashed line, respectively. Lower panel: the Co^{2+} quartet and doublet spin states are represented as a solid line and a dashed line, respectively.

Another important issue of our procedure is the optimization of the effective radii (ρ_M) used in the CPCM to build the cavities occupied by the solute in the solvent by means of interlocking spheres centered on atoms. Each sphere forming the solute cavity is subdivided into finite elements (tesserae): while in the original procedure 60 tesserae were used for each sphere, more stable results are obtained by using elements with constant average area. In the present study we have used an average area of 0.2 Å, resulting in about 240 tesserae for a typical sphere. In our approach we have retained the standard CPCM radii of oxygen and hydrogen (1.68 and 1.44 Å, respectively) while optimizing the ion radii. This last task has been accomplished by following a

(19) Barone, V.; Cossi, M. *J. Phys. Chem. A* **1998**, *102*, 1995.
(20) Cossi, M.; Barone, V. *J. Chem. Phys.* **1998**, *109*, 6246.
(21) Klamt, A.; Schürmann, A. G. *J. Chem. Soc., Perkin Trans. 2* **1993**, 799.
(22) Baldridge, K.; Klamt, A. *J. Chem. Phys.* **1997**, *106*, 6622.
(23) Cossi, M.; Rega, N.; Scalmani, G.; Barone, V. *J. Chem. Phys.* **2001**, *106*, 6622.
(24) Hay, P. J.; Wadt, W. R. *J. Chem. Phys.* **1985**, *82*, 270.
(25) Wadt, W. R.; Hay, P. J. *J. Chem. Phys.* **1985**, *82*, 284.
(26) Hay, P. J.; Wadt W. R. *J. Chem. Phys.* **1985**, *82*, 299.
(27) Breneman, C. M.; Wiberg, K. B. *J. Comput. Chem.* **1990**, *11*, 361.
(28) Becke, A. D. *J. Chem. Phys.* **1992**, *96*, 2155.
(29) Parr, R. G.; Yang, W. *Density Functional Theory of Atoms and Molecules*; Oxford University Press: New York, 1989.
(30) Wilson, A.; van Mourik, T.; Dunning, T. H., Jr. *J. Mol. Struct. (THEOCHEM)* **1996**, *388*, 339.

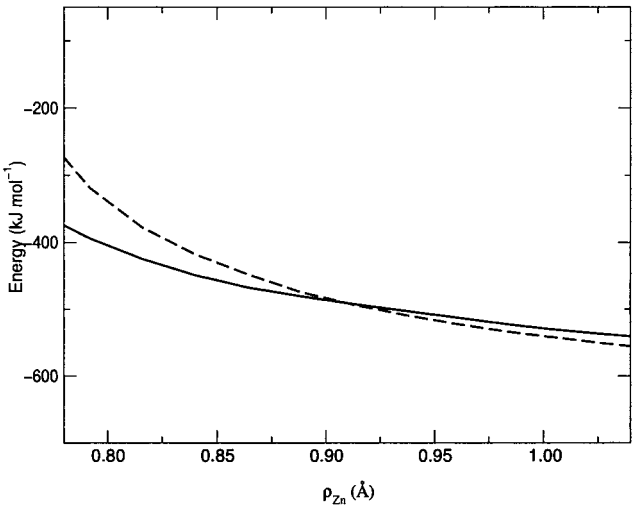

Figure 3. Cavity radius optimization curve for the Zn^{2+} ion. The U_{WMW} (solid line) and $2U_{WM} + U_{WW}$ (dashed line) energies are plotted as a function of the effective radius ρ_{Zn}.

Table 3. Calculated Values of the Radius ρ_M for the Zn^{2+}, Ni^{2+}, and Co^{2+} Ions[a]

ion	ρ_M(present), Å	ρ_M(REF), Å
Zn^{2+}	0.904	1.040
Ni^{2+}	1.020	1.110
Co^{2+}	1.062	

[a] Data in column "REF" are from ref 5.

previously proposed procedure,[4] which is based on the observation that an effective pair potential may also be extracted from calculations on $M^{n+}-(H_2O)_m$ clusters in which $m - 1$ water molecules are fixed at suitable coordination sites and the position of the mth water molecule is varied. Application of the CPCM allows the use of $m = 2$ for the determination of the ion effective radius and $m = 1$ for the subsequent PES generation.

The ion effective radii can be fixed by running two sets of energy calculations on the $M^{n+}-(H_2O)$ and $M^{n+}-(H_2O)_2$ clusters with variable ρ_M values. From the second set of results we can get the water−ion−water potential U_{WMW} in the form:

$$U_{WMW} = \langle\psi|\hat{\mathscr{H}}^{(0)}|\psi\rangle_{WMW} - \langle\psi|\hat{\mathscr{H}}^{(0)}|\psi\rangle_M - 2\langle\psi|\hat{\mathscr{H}}^{(0)}|\psi\rangle_W \quad (2)$$

Then, if the perturbation due to the polarizable continuum solvent is of the right magnitude, we should have:

$$U_{WMW} = 2U_{MW} + U_{WW} \quad (3)$$

where U_{WW} is the water−water potential not containing the effect of the electric field of the ion, and U_{MW} is given by eq 1. Both sides of eq 3 depend on the radius ρ_M, but U_{MW} is much more sensitive than U_{WMW} to this parameter. Therefore, this equation is satisfied only for a specific value of ρ_M, which is then adopted in all the calculations.

As an example, Figure 3 shows the results of the Zn^{2+} radius optimization obtained for a Zn−O distance of 2.2 Å and a O−Zn−O angle of 90°. Note that in this case the quantities of eq 3, namely U_{WMW} and $2U_{MW} + U_{WW}$, coincide when ρ_{Zn} is equal to 0.904 Å.

However, we should point out that it was not possible to obtain the optimized ρ_M values for the Ni^{2+} and Co^{2+} ions, with the same accuracy. In fact, due to numerical noise in the calculation of the $\langle\psi|\hat{\mathscr{H}}^{(0)}|\psi\rangle_M$ term for ρ_M below 1.08 Å, we had to extrapolate the ion cavity sizes from the data at longer ρ_M values. In Table 3 a summary of the calculated and, where available, published ρ_M values is reported.

Note that there is a significant difference between our results and those published by others.[5] This is not surprising, since solvation energies depend on the basis set simply because the solute electron distribution changes. In particular the charge separation decreases when the basis set is enlarged, and the same occurs to the solvation energies, this effect being larger for U_{MW} than for U_{WMW}. As a consequence, the metal radii satisfying eq 3 are generally smaller for larger basis sets. For instance using a 6-31G(d,p) basis set, the Zn^{2+} radius becomes 0.965 Å, significantly closer to the result obtained in ref 5 with a DZP basis set. Since our choice of the water basis set (cc-pVTZ) provides charges very close to SPC/E ones (see Table 1) we are confident in our effective radii for metal ions. The importance of the ion cavity size in the first step of our numerical procedure can be appreciated from the results of the MD simulations. As a matter of fact, our Zn^{2+} ion cavity radius (0.904 Å) leads to a $Zn^{2+}-O$ distance (2.08 Å) for the water molecules in the first hydration shell in excellent agreement with the EXAFS value (2.078 Å, see Table 5), whereas use of the radius proposed in ref 5 (1.04 Å) leads to a slightly overestimated value (2.09 Å).

A last important factor in this first step of our computational scheme is the choice of the grid used for the generation of the quantum mechanical energies to be fitted. As sketched in Figure 1, we adopted an internal coordinate system of reference and spanned the ab initio calculations over a wide range. In particular, we kept fixed the water geometry during the PES calculation and we carried out the energy calculations for ion−water distances in the range $1.2 < R_{MO} < 4.0$ Å and for ∠MOH angles in the range of $37.745° < \angle MOH < 127.745°$, while keeping the ion coplanar with the water molecule. The step sizes of the internal variables were 10° for θ and 0.02 Å for R_{MO}, giving rise to a grid of 1400 points, which were sufficient to obtain a very good fitting with the effective two-body potentials described in the next section. We must point out that several numerical problems occurred during the PES evaluation, in particular in the repulsive and long-range interaction regions. In fact, while in the short R_{MO} distance range we were able to avoid curve crossing already for the bare ion−water system, in the long distance region only use of PCM removed the *curve-jumping* between close electronic states plaguing in vacuo computations.

2.2. Step II: Potential Parameters Evaluation. The ion−water interaction energies obtained from the ab initio potential scans were fitted by using the following analytic function:

$$V = \frac{q_i q_o}{r_{io}} + \frac{A_o}{r_{io}^4} + \frac{B_o}{r_{io}^6} + \frac{C_o}{r_{io}^8} + \frac{D_o}{r_{io}^{12}} + E_o e^{-F_o/r_{io}} + \sum_{ih=ih1,ih2} \frac{q_i q_h}{r_{ih}} + \frac{A_h}{r_{ih}^4} + \frac{B_h}{r_{ih}^6} + \frac{C_h}{r_{ih}^8} + \frac{D_h}{r_{ih}^{12}} \quad (4)$$

where r_{io}, r_{ih1}, and r_{ih2} are the ion−solvent distances; q_i, q_o, and q_h are the electrostatic charges of the system; A_o, ..., F_o, A_h, ..., and D_h are the unknown parameters. We chose to adopt this function, already used for metal ion−water interactions,[5] even though only in the case of Ni^{2+} all ten parameters were necessary for the best fitting, while nine parameters were needed for Zn^{2+} and Co^{2+}, where D_h was equal to zero.

As mentioned, the water charges were kept fixed to the SPC/E values, while q_i was equal to 2 au for all three ions. The fitting was carried out by using the Newton method as implemented in the statistic package SAS.[31] The Newton iterative method is used to solve systems of nonlinear equations,[32] and it works by regression of the residuals onto a function of the first and second derivatives of the model with respect to the parameters, until the estimates converge. In contrast to other available nonlinear fitting methods (Steepest-descend, Marquardt, etc.) the Newton one uses the Hessian with respect to the parameters, thus

(31) SAS/STAT User's Guide, Version 6.12, SAS Institute Inc.: Cary, 2000.
(32) Bard, J. *Nonlinear Parameter Estimation*; Academic Press: New York, 1974.

Table 4. Ion−Water Interaction Parameters and Corresponding Standard Deviations of Eq 4.

parameters	Zn^{2+} (std dev)	Ni^{2+} (std dev)	Co^{2+} (std dev)
A_o	2.049×10^{-2} (1.1×10^{-2})	-3.861×10^{-1} (9.3×10^{-2})	3.790×10^{-2} (6.5×10^{-2})
B_o	2.910×10^{-2} (1.3×10^{-3})	6.985×10^{-2} (9.0×10^{-3})	3.593×10^{-2} (5.3×10^{-3})
C_o	-2.834×10^{-4} (1.7×10^{-5})	-8.618×10^{-4} (1.2×10^{-4})	-4.006×10^{-4} (6.8×10^{-5})
D_o	8.011×10^{-9} (8.4×10^{-10})	3.538×10^{-8} (5.7×10^{-9})	1.351×10^{-8} (3.1×10^{-9})
E_o	$-3.633 \times 10^{+4}$ ($2.0 \times 10^{+3}$)	$-6.686 \times 10^{+4}$ ($1.5 \times 10^{+4}$)	$-3.252 \times 10^{+4}$ ($6.7 \times 10^{+3}$)
F_o	23.601 (1.7×10^{-1})	24.077 (7.1×10^{-1})	21.892 (8.1×10^{-1})
A_h	8.377×10^{-2} (1.8×10^{-3})	1.119×10^{-1} (4.3×10^{-2})	3.606×10^{-2} (8.0×10^{-4})
B_h	-1.563×10^{-3} (6.1×10^{-5})	-8.688×10^{-4} (2.3×10^{-3})	1.584×10^{-5} (5.0×10^{-6})
C_h	1.244×10^{-5} (5.3×10^{-7})	-1.677×10^{-5} (3.7×10^{-5})	1.000×10^{-8} (1.0×10^{-10})
D_h		9.748×10^{-10} (2.8×10^{-9})	−

Table 5. Parameters of the Fitted Minimum Energy Curves[a]

ion	R_{MO} (Å)	ΔE_{min} (kJ mol^{-1})	R_{exp} (Å)
Zn^{2+}	1.95	−245	2.078
Ni^{2+}	1.95	−290	2.072
Co^{2+}	2.00	−265	2.092

[a] ΔE_{min} is the minimum value of the minimum energy curves, R_{MO} is the corresponding M^{2+}−O distance, and R_{exp} is the M^{2+}−O first shell distance determined from the EXAFS analysis.[33]

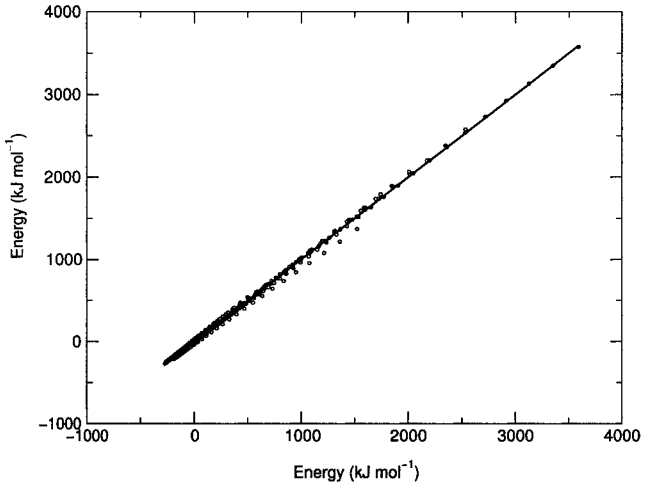

Figure 4. Fitted vs calculated energy points of the Co^{2+}−water pair potential.

allowing the error minimum to be reached more efficiently and with higher precision.

To evaluate the resulting fitting function, a comparison between ab initio calculated and fitted energies for our Co^{2+}−H_2O force field is shown in Figure 4. From this figure it is evident that the agreement between the fitting function and the original quantum mechanical data is very good. In particular, the standard deviations for all the data sets are 2.9, 17.5, and 16.1 kJ mol^{-1} for Zn^{2+}, Ni^{2+}, and Co^{2+}, respectively. The final ion−water interaction parameters for Zn^{2+}, Ni^{2+}, and Co^{2+} are reported in Table 4, including the standard deviations for each parameter. As already mentioned, the best fitting of the Zn^{2+} and Co^{2+} curves was obtained without the use of the D_h parameter.

Figure 5 shows the fitted energy curves for the ion−water minimum configuration as a function of the ion−O distance. A first check of the reliability of the described procedure can be performed by comparing the trend of these three curves with the EXAFS experimental results in ref 33. Note that the energy curve associated with the Ni^{2+} ion is shifted toward lower values with respect to the other two ions, in agreement with the well-known higher stability of its aqua complex. As far as the Zn^{2+} and Co^{2+} ions are concerned, the energy curves of Figure 5 show an intersection point at about 1.75 Å. In the distance region below this value the Zn^{2+} curve is more negative than the Co^{2+} one, while an opposite trend can be observed in the distance region above. As a result, the Co^{2+} ion presents a more negative value of the

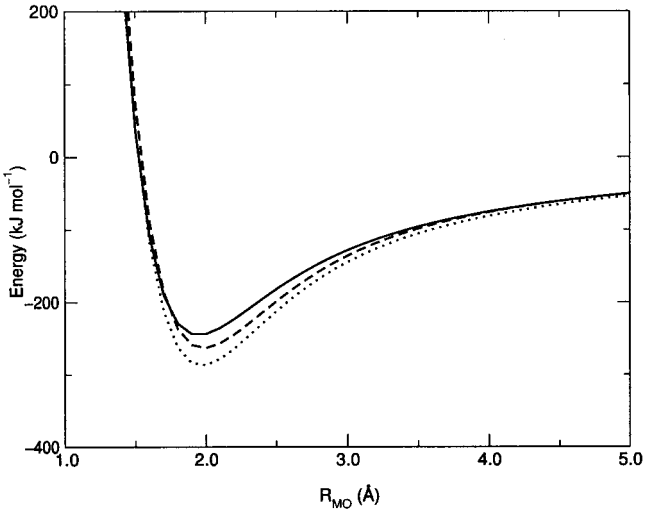

Figure 5. Fitted energy curves of the ion−water minimum configuration as a function of the R_{MO} ion−oxygen distance. The solid line refers to the Zn^{2+}−H_2O, the dashed line to the Co^{2+}−H_2O, and the dotted line to the Ni^{2+}−H_2O complexes, respectively.

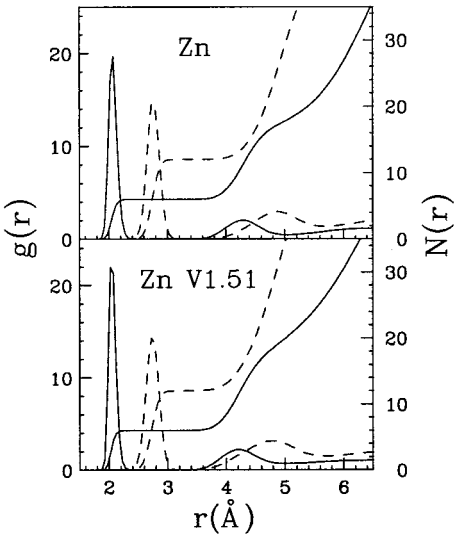

Figure 6. Radial distribution functions and corresponding running integration numbers for Zn−O (solid line) and Zn−H (dashed line) obtained from the MD simulations using our ab initio effective pair potentials (upper panel) and using the original GROMACS potentials (lower panel).

minimum energy as compared to Zn^{2+}. This finding is in agreement with the EXAFS experimental results reported in ref 33 which show the existence of a more stable aqua complex in the case of the Co^{2+} ion, as compared to Zn^{2+}. It is interesting to stress that our model correctly reproduces the experimental finding that the Co^{2+} hydration shell is more stable than the Zn^{2+} one, but the Co−O coordination distance is longer (see Table 5 and ref 33).

2.3. Step III: Molecular Dynamics. The Zn^{2+}, Ni^{2+}, and Co^{2+} water potentials obtained from the previously described procedure (see Table 4) have been included in the GROMACS package version 1.51.[18] Three MD simulations have been performed using these potentials for the ion−water interactions and the SPC/E model for the water−water interactions. The simulated systems consisted of one ion and 819 SPC/E water molecules. A further simulation was performed with the Zn^{2+}−water original GROMACS interaction potential to compare structural results. A cutoff of 12 Å was used for the pair interactions, updating the neighboring pair list every 10 steps. According to Perera et al.[34] use of the simple truncation method, when applied to simulations with only one ion, produces a solvation structure very similar to that obtained from simulations where Ewald or reaction field methods are used. This approximation is particularly valid for 3d divalent ions which tightly bound the first shell water molecules. The temperature was kept fixed at 300 K by weak coupling to an external temperature bath with a coupling constant of 0.1 ps.[35] The systems were equilibrated for 50 ps and simulated for 1 ns with a time step of 2 fs. The trajectories were saved every 25 time steps for analyses, which were carried out using in-house written codes. The ion−water radial distribution functions $g(r)$'s were averaged over 1 ns after equilibration. The coordination numbers N of the ions were calculated by using the following relation:

$$N = 4\pi\rho \int_0^{R_{\min}} g(r) r^2 \, dr \tag{5}$$

where $R_{\min}$ is the first minimum of the $g(r)$ and ρ is the atomic density of the system.

The residence times τ_N of water molecules in the coordination shells of the ions have been measured following the method of Impey et al.[36] According to this procedure it is possible to define for each water molecule a survival probability function $P_j(t, t_n, t^*)$. This is a binary function that takes the value *one* if the water molecule j lies within the referred hydration shell at both time steps t_n and $t + t_n$ and does not leave the coordination shell for any continuous period longer than t^*. Otherwise, it takes the value *zero*. From P_j it is possible to define an average quantity $n_{\text{ion}}(t)$ given by the expression:

$$n_{ion}(t) = \frac{1}{N_t} \sum_{n=1}^{N_t} \sum_j P_j(t_n, t, t^*) \tag{6}$$

where N_t is the total number of steps. Taking into account the first coordination shell, $n_{\text{ion}}(0)$ provides a further definition of the coordination number. At long times, $n_{\text{ion}}(t)$ decays in an exponential fashion, with a characteristic correlation time τ_{ion} which defines the residence time of the water molecule in the shell. We have chosen a t^* value equal to the time interval between saved configurations (25 fs). The residence times of water molecules in the second hydration shells were calculated without including the water molecules belonging to the first coordination shell.

3. Results and Discussion

Figure 6 shows the Zn−O and Zn−H $g(r)$'s obtained from our ab initio potential and from the GROMACS original Zn^{2+}−water pair interaction functions. From this figure it is evident that the Zn−O and Zn−H $g(r)$'s obtained from the two sets of potentials are quite similar. In both cases the integration over the Zn−O and Zn−H first peaks gives coordination numbers of six and twelve, respectively, in agreement with the existence of an octahedral structure around the ion. Note that the existence of an octahedral hydration shell has not been assumed "a priori" in our procedure, but it has been derived from the MD simulations. Therefore, our method can be successfully applied to investigate less well-characterized ionic solutions when structural and dynamic experimental results are contradictory. The Zn−O and Zn−H $g(r)$'s show very sharp and separated first peaks with a well-defined depletion zone between the first and second hydration shells. This indicates the existence of a well-ordered nearest-neighbor coordination structure and the presence of a preferential orientation of water molecules in the first hydration shell. A similar result has been obtained for the Ni^{2+} and Co^{2+} water solutions and the corresponding ion-O and ion-H $g(r)$'s are shown in Figure 7.

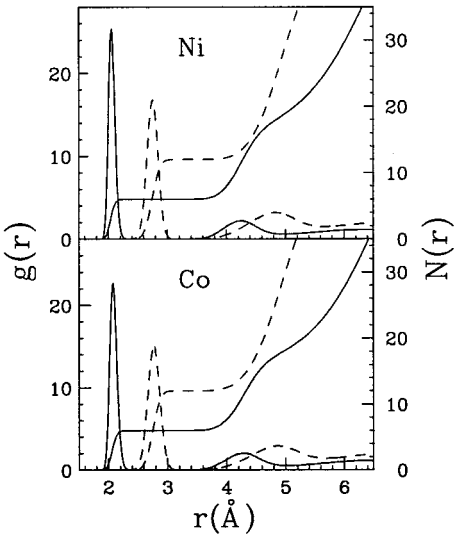

Figure 7. Radial distribution functions and corresponding running integration numbers for Ni^{2+} (upper panel) and Co^{2+} (lower panel). The M−O $g(r)$'s are represented by full lines and the M−H $g(r)$'s by dashed lines.

It is well-known that the EXAFS technique provides very accurate structural results on the first hydration shell, which are independent from the MD starting models. For this reason, comparison of radial distribution functions derived from MD simulations and from EXAFS data provides a useful test of the reliability and accuracy of the whole procedure used for the potential generation. A thorough description of a method that combines MD and EXAFS results and its application to the structural investigation of Zn^{2+}, Ni^{2+}, and Co^{2+} aqueous solutions can be found in ref 33.

The Zn−O $g(r)$ distribution obtained from the EXAFS data analysis and the results of the MD simulations performed with both our and GROMACS potentials are shown in the upper panel of Figure 8. Both the MD $g(r)$'s are in good agreement with the EXAFS experimental results and the first shell distance obtained from our procedure coincides with the experimental value (2.078 Å), within the reported error, while the GROMACS potential produces a slightly shorter value (2.063 Å). The EXAFS Zn−O first neighbor peak is found to be less asymmetric than predicted by MD, and its rise is less steep. The most evident effect is that a much smaller value of the root-mean-square variation σ is obtained from the MD simulations (0.069 and 0.060 Å for our potential and for the original GROMACS one, respectively) as compared to the EXAFS experimental determination (0.093 Å). Similar results were

(33) D'Angelo, P.; Barone, V.; Chillemi, G.; Sanna, N.; Meyer-Klaucke, W.; Pavel, N. V. *J. Am. Chem. Soc.* **2002**, *124*, 1958−1967.
(34) Perera, L.; Essmann, U.; Berkowitz, M. L. *J. Chem. Phys.* **1995**, *102*, 450.
(35) Berendsen, H. J. C.; Postma, J. P. M.; Di Nola, A.; Haak, J. R. *J. Chem. Phys.* **1984**, *81*, 3684.
(36) Impey, R. W.; Madden, P. A.; McDonald, I. R. *J. Phys. Chem.* **1983**, *87*, 5071.

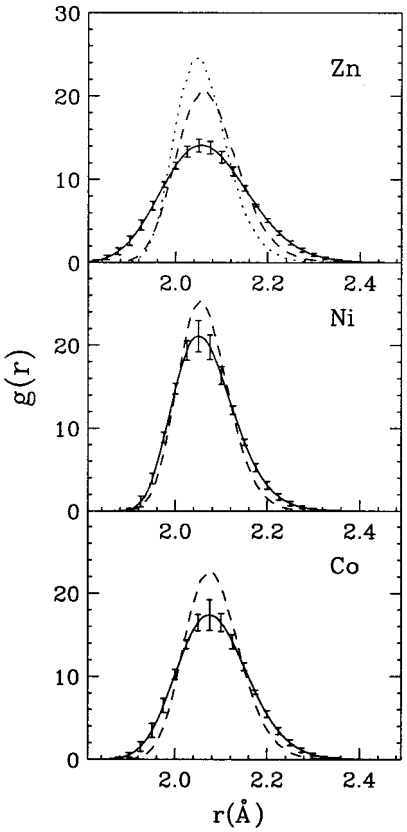

Figure 8. M−O $g(r)$'s from EXAFS analysis (solid line) and MD simulations with our potential (dashed line) for Zn^{2+} (upper panel), Ni^{2+} (middle panel), and Co^{2+} (lower panel). The Zn−O $g(r)$ obtained from MD simulation with the original GROMACS potential is also reported in the upper panel (dotted line).

obtained by Kuzmin et al.,[37] and this discrepancy was attributed to the simplicity of the Lennard-Jones potential function used in their calculations. According to our opinion this effect is only partially due to the analytical expression of the ion−water interaction function used in the simulations, as our more accurate potential provides improved results but is still not able to completely reproduce the experimental data. The results obtained for the Ni^{2+} and Co^{2+} water solutions are shown in the middle and lower panels of Figure 8, respectively. In these cases the MD $g(r)$'s are in much better agreement with the EXAFS results, showing the accuracy of the calculations. This finding suggests that the discrepancy on the σ values observed for the Zn^{2+} ion is most probably due to the water−water interaction parameters and to the rigidity of the water model used in the simulations. Moreover, the mean-square variation parameters obtained from the EXAFS data are influenced by the migration of water molecules between the first and second hydration shell. This effect is not accounted for in our MD simulations. It is worth noting that the best agreement is obtained for Ni^{2+}, which possesses a quite stable hydration sphere thus being less sensitive to this effect. A previous MD and EXAFS investigation on the Ni^{2+}−water system has been carried out[38] and the MD Ni−O $g(r)$ obtained is very similar to the one determined from our calculations. A thorough comparison between the ion−H and ion−O first shell structural parameters obtained from our MD simulations and X-ray diffraction (XRD) and neutron diffraction

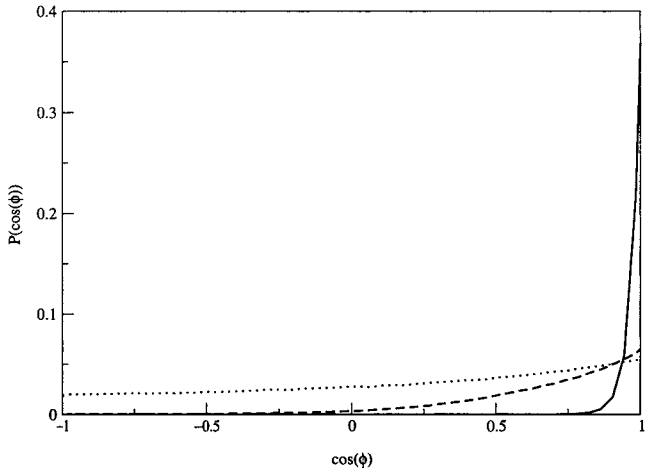

Figure 9. Probability distribution of the cosine of the tilt angle ϕ between the ion−O direction and the water dipole moment, for Co^{2+} first (solid line) and second (dashed line) hydration shell, and for bulk water molecules (dotted line).

experimental investigation can be found in ref 33. The agreement between the MD and diffraction data further enforces the reliability of the entire procedure.

The higher distance structural picture that results from the MD simulations is as follows. The second coordination shells are composed of 12−13 water molecules in a distance range between 3.6 and 5.0 Å. The ion−O $g(r)$'s show second shell peaks at a mean distance of 4.28 Å. As already mentioned, reliable structural information on the second hydration shell cannot be gained from the EXAFS technique. In the past years a number of XRD studies have been carried out on Zn^{2+}, Ni^{2+}, and Co^{2+} aqueous solutions.[1,39−41] The second shell mean distances obtained by our calculations are in very good agreement with the XRD ones. Note that the number of water molecules in the second hydration shell as determined from XRD measurements is usually twice the number of water molecules in the first shell. This result is consistent with our determination.

The experimental values of the residence times of water molecules in the first hydration shell of Zn^{2+}, Ni^{2+}, and Co^{2+} aqueous solutions are in the range 10^{-5}−10^{-8} s, more than 1 order of magnitude longer than our simulation time (1 ns).[42] This finding was confirmed by our calculations as no water molecules exchanged with the bulk during the nanosecond of simulation. Note that our potential does not treat differently the water molecules in the first shell and in the bulk. The residence times of water molecules in the second hydration shells were calculated considering a distance cutoff of 5.0 Å for all three systems and the determined values were 3.4, 10.3, and 4.5 ps for Zn^{2+}, Ni^{2+}, and Co^{2+}, respectively. Longer residence times have been obtained, as expected, for the Ni^{2+} ion which forms the most stable hydration complex.[42]

The orientation of water molecules around the ions is described by the cosine of the tilt angle ϕ between the ion−O direction and the water dipole moment (see Figure 1). The corresponding distributions $P(\cos\phi)$ are shown in Figure 9, as

(37) Kuzmin, A.; Obst, S.; Purans, J. *J. Phys.: Condens. Matter* **1997**, *9*, 10065.
(38) Wallen, S. L.; Palmer, B. J.; Fulton, J. L. *J. Chem. Phys.* **1998**, *108*, 4039.
(39) Radnai, T.; Pálinkás, G.; Caminiti, R. *Z. Naturforsch.* **1982**, *37a*, 1247.
(40) Caminiti, R.; Cucca, P.; Monduzzi, M.; Saba, G. *J. Chem. Phys.* **1984**, *81*, 543.
(41) Caminiti, R. *J. Chem. Phys.* **1986**, *84*, 3336.
(42) Miyanaga, T.; Sakane, H.; Watanabe, I. *Bull. Chem. Soc. Jpn.* **1995**, *68*, 819.

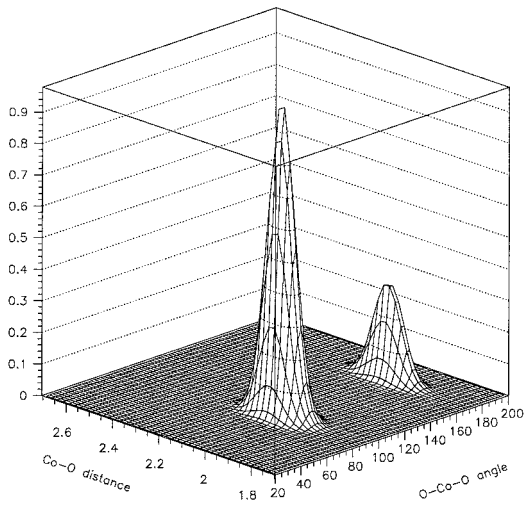

Figure 10. Representation of the O−Co−O three-body distribution as a function of the O−Co−O angle θ and one of the two symmetric Co−O distances in Å.

an example, for three different Co^{2+}−O range distances which correspond to the first and second hydration shells, and to the bulk water molecules in the range distance between 8 and 9 Å. The tilt angle distributions have been calculated by using cos ϕ steps of 0.002 and integration of each curve provides the coordination number of each shell (6, 12, and 30 for the first shell, second shell, and bulk water molecules, respectively). Similar results have been obtained for Zn^{2+} and Ni^{2+}. The water molecules in the first hydration shell show a quite sharp distribution centered around cos $\phi = 1$, i.e., the ion, oxygen, and two hydrogen atoms lie in one plane in a so-called "dipole" configuration. The sharpness of the $P(\cos \phi)$ curves in the first hydration shell accounts for the strong structuring ability of the three ions. Water molecules in the second hydration shell show, obviously, a less sharp distribution but a relatively strong structure is maintained also in this distance range. At longer distances all the possible ion−water configurations are populated, even though a preferential orientation can still be observed.

Finally, the three-dimensional arrangements of the water molecules around the ions have been characterized in terms of the O−ion−O and ion−$O_{1st\ shell}$−$O_{2nd\ shell}$ triangular configurations. The analysis of the three-body distributions of the Zn^{2+}, Ni^{2+}, and Co^{2+} water solutions is an essential starting point for the correct interpretation of the multiple scattering effects present in the EXAFS spectra. From these analyses, performed with grids of 0.05 Å and 5°, the existence of well-defined peaks in the O−ion−O triangular configurations has been singled out for all three ions. These peaks are characterized by trivariate normal distribution functions with negligible distance−angle and distance−distance correlations. Integration of these peaks allowed the number of triangular configurations contributing to the distribution to be estimated. A three-dimensional representation of the O−Co−O distribution as a function of the O−Co−O angle θ and one of the two symmetric Co−O distances is reported in Figure 10 as an example. Similar distributions have been obtained for Zn^{2+} and Ni^{2+}. In all cases the O−ion−O distributions show two peaks at $\theta \simeq 90°$ and 180° in agreement with the expected octahedral coordination of these ions. The structural parameters defining all the $g(r_1, r_2, \theta)$ three-body distributions are listed in Table 6. The ion−$O_{1st\ shell}$−$O_{2nd\ shell}$ three-body distributions obtained from our calculations are

Table 6: Parameters of the O−Ion−O and Ion−$O_{1st\ shell}$−$O_{2nd\ shell}$ $g(r_1,r_2,\theta)$ Three-Body Distributions[a].

first peak	O–Zn–O	O–Ni–O	O–Co–O
R_{MO}	2.07	2.06	2.06
$\sigma_{R_{MO}}$	0.068	0.055	0.055
θ	173°	174°	174°
σ_θ	4°	4°	4°
N	3	3	3
second peak	**O–Zn–O**	**O–Ni–O**	**O–Co–O**
R_{MO}	2.07	2.06	2.06
$\sigma_{R_{MO}}$	0.068	0.055	0.055
θ	90°	90°	90°
σ_θ	5°	5°	5°
N	12	12	12
	Zn–O–O	**Ni–O–O**	**Co–O–O**
R_{MO}	2.07	2.06	2.08
$\sigma_{R_{MO}}$	0.068	0.056	0.061
R_{OO}	2.75	2.74	2.75
$\sigma_{R_{OO}}$	0.130	0.127	0.131
θ	126°	124°	125°
σ_θ	13°	13°	13°
N	17	19	18

[a] The $g(r_1,r_2,\theta)$'s are described by trivariate normal distribution functions. In the case of the O−ion−O distributions only one of the two symmetric ion−oxygen distances (R_{MO}) is reported. Distances and root mean square variations (σ) are given in Å.

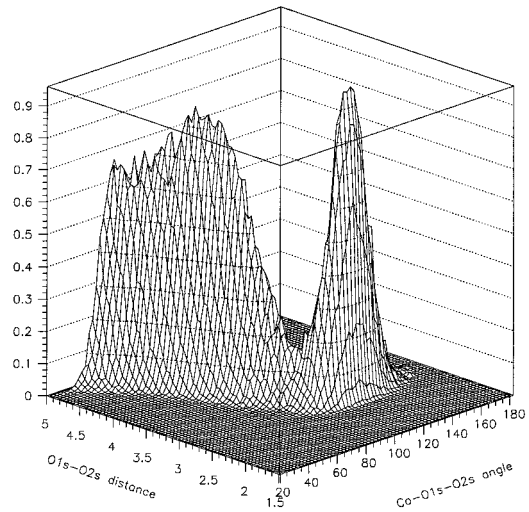

Figure 11. Representation of the Co−$O_{1st\ shell}$-$O_{2nd\ shell}$ three-body distribution as a function of the $O_{1st\ shell}$−$O_{2nd\ shell}$ distance (Å) and Co−$O_{1st\ shell}$−$O_{2nd\ shell}$ angle θ, at the Co−$O_{1st\ shell}$ distance of 2.10 Å.

similar for the three ions and the Co−$O_{1st\ shell}$−$O_{2nd\ shell}$ $g(r_1, r_2, \theta)$ is shown in Figure 11, as an example. This distribution is a function of the $O_{1st\ shell}$−$O_{2nd\ shell}$ distance and of the Co−$O_{1st\ shell}$−$O_{2nd\ shell}$ angle θ, while the Co−$O_{1st\ shell}$ distance has been kept fixed at 2.10 Å, which corresponds to the $g(r)$ first shell maximum. All three distributions show a peak at $R_{OO} \simeq$ 2.75 Å with a maximum located at about 125°. For low θ values the oxygen atoms of the second shell lie in a quasieclipsed configuration. This situation is described by a broad, $\theta - R_{OO}$ correlated peak, extending from 0° to 90°. Due to the high broadness of the distribution, this peak has not been considered in the EXAFS data analysis, while the peak centered at 125° could give rise to a not-negligible multiple scattering contribution. All the details concerning the EXAFS data analysis of these systems, including the three-body correlation functions, are described in ref 33.

4. Conclusions

In this paper we have introduced and validated a general and effective computational procedure for the study of ionic species in liquid solutions by MD simulations using effective two-body potentials. This procedure has allowed, for the first time, the development of the Co^{2+}−water potential function that permitted us to obtain reliable structural information by means of MD simulation of the ion in aqueous solution. Due to the open shell nature of the Co^{2+} electronic state, we had largely revised the original ab initio procedure of Floris et al.[4,5] and the new improved approach has been validated by comparing the MD Zn− and Ni−water structural and dynamical properties with experimental results. Moreover, Ni−H, Zn−H, and Co−H interactions were included in the force field allowing MD structural information on the ion−H $g(r)$'s to be obtained. Comparison of MD and EXAFS results shows the reliability of the model concerning first solvation-shell structural parameters. At the same time MD results for the second solvation shells are in agreement with XRD data and provide a valuable aid for the interpretation and fitting of EXAFS results. Together with its intrinsic interest, the example of transition metal ions paves the route for more ambitious targets, like e.g. heavy metals and/or nonaqueous solvents. Preliminary investigations on the Cd^{2+}−water system show that this procedure can be successfully applied also to different ions. Since the whole computational procedure is performed by using commercial codes and can be considered as a user-friendly "black-box" it opens interesting perspectives also for the analysis and interpretation of experimental results by nonspecialists.

Acknowledgment. This work was sponsored by the Italian Research Council (CNR), by the Italian Ministry for the University and the Scientific and Technological Research (MURST), and by Gaussian Inc. We thank M. Scarnò for helpful suggestions and the CASPUR computational center for providing the computer architectures used in this work.

JA015686P